

Investigating the effect of Madden-Julian Oscillation on the frequency of dust storms in the west of Iran

Bromand Salahi ^{1*}, Fatemeh Vatanparast Ghaleh Juq ² and Mohammadreza Nazari Radsani³

¹Professor, Department of Physical Geography, University of Mohaghegh Ardabili, Ardabil, Iran

²Ph.D. Student, Department of Physical Geography, University of Mohaghegh Ardabili, Ardabil, Iran

³M.Sc. Graduate in Water Sciences and Engineering- Agricultural Meteorology, Shiraz University, Shiraz, Iran

(Received: 26 January 2023, Accepted: 28 March 2023)

Abstract

Deserts and semi-desert countries have become increasingly affected by dust storms in recent years. In this research, the effect of the real-time multivariate of the Madden-Julian Oscillation (MJO) index on the frequency of dust storms in the west of Iran (Sarpol-E-Zahab, Islamabad Gharb, Kermanshah, and Kangavar stations located in Kermanshah province) during February–July for the period 1987-2022 and the frequency percentage of this index for Phases 7-2 (7, 8, 2 and 1) and Phases 3-6 (3, 4, 5 and 6) were investigated. The results of the analysis of the relationship between the MJO and dust storms showed that between 57 and 75% of dust storms occurred in phases 7-2 of the MJO and 25 to 42% in phases 3-6. Phases 7-2 of the MJO have a higher percentage of dust storms than phases 3-6. According to the results of the Mann-Whitney test, the displacement of phases 7-2 and phases 3-6 of the MJO have significantly led to dust storms at the Kermanshah and Kangavar stations. Due to the suitability of the HYSPLIT model for tracking dust storms, the paths of dust entering Kermanshah province were investigated with this model. Tracking the paths of dust entering Kermanshah province with the HYSPLIT model and analyzing the wind speed and direction maps of 850 hPa level indicate an increase in the speed of westerly winds. The increase in the speed of westerly winds and the decrease in soil moisture in phases 7-2 and 3-6 have caused the movement of dust particles from Iraq, eastern parts of Syria, and Khuzestan province to the studied area.

Keywords: Madden-Julian Oscillation (MJO), dust storm, Kermanshah province, Mann-Whitney test, Hysplit model

1 Introduction

Dust and sand storms involve weather conditions with strong winds that cause dust and sand to rise and disperse, resulting in reduced horizontal visibility to less than 1 km and air pollution (Goudie and Middleton 2006; Mei et al. 2008). Dust storms are a significant natural hazard to human health and can depopulate some areas (Mesbahzadeh et al. 2020). In recent years, dust pollution has become a serious environmental problem and many countries adjacent to the dust source areas have faced it. (Saeed, et al. 2014; Chauhan et al. 2018; Gui et al. 2022). Dust events often occur in arid and semi-arid regions of the world, such as the Middle East, Europe, Latin America, North America, Australia, and East and South Africa (Gao et al. 2012; Yong et al. 2020; Shao et al. 2011). The Middle East has many dust storms originating from the Arabian Peninsula, Syria, Egypt, Iraq, and Iran. Research shows that in the last decade, the occurrence of dust phenomena has increased to the west and southwest of Iran (Farhadipour et al. 2018). Kermanshah province is located in the Zagros region, which has faced vegetation destruction due to factors, such as war, population scale-up, deforestation, and overgrazing (Ahmadi Doabi et al. 2017; Azizi et al. 2012). Due to the common border, a huge amount of Iraq dust storms arrive in Kermanshah province. Because of internal and external dust storm sources in this province, it is necessary to carry out various investigations in this regard to prevent the occurrence and severity of this phenomenon (Karimi et al. 2018). The MJO is one of the dominant climate change patterns in tropical marine climate, which plays an essential role in the atmosphere-ocean cycle system. The MJO, characterized by eastward propagation, is a coupled large-scale convection-atmospheric circulation system on intraseasonal time scales that has an important function in the

interrelationship of climate systems (Zhang 2005; Zhang 2013). Reproducing the MJO is an essential issue in atmospheric general circulation models (Ahn et al. 2020; Hung et al. 2013; Ling et al. 2017; Ling et al. 2019; Salahi et al. 2024).

Many studies have been conducted to improve our understanding of the conditions of dust storms and their movement processes. Gong et al. (2006) showed a negative correlation between dust and Arctic Oscillation (AO) in North China. Xu et al. (2007) showed a significant inverse correlation between dust particles and winter NAO in the Tibetan Plateau. Gong et al. (2007) found that dust storm frequency in northern China is significantly correlated to the Pacific North American (PNA) pattern with a Pearson's correlation coefficient of +0.60 on the interannual time scale during 1962–2002. Ragsdale et al. (2013) examined the variability of PM₁₀ particles in Santiago, Chile, based on the MJO phases, and concluded that the highest PM₁₀ concentration occurs in phase 4 of the MJO. Guo et al. (2013) investigated the changes in dust and aerosol in the Atlantic Ocean concerning the MJO. Lee et al. (2014) investigated the combined effect of ENSO with the AO negative phase on dust source activity in North China from 1961 to 2002. The results showed significant enhancement dust in the negative phase of AO along with El Niño. Banerjee and Kumar (2016) investigated the effect of Enso on dust particle variability in the northwest Indian Ocean from April to August. The results showed that La Niña leads to more dust production, while the amount of dust during El Niño will decrease

Research by Yu and Ginoux (2021) in Australia showed that peak dust activity in phases 1 to 6 of the MJO is associated with El Niño activity. Li et al. (2021) evaluated the effect of El Niño-Southern Oscillation (ENSO) on dust in different regions of the

world in the statistical period of (1982-2019). They showed that the dust concentration is positively related to ENSO. They also showed that the La Niña event is associated with an accretion of dust concentration and an El Niño event with a decline in the dust concentration. Labban and Butt (2021) investigated the relationship between dust storms in Saudi Arabia with meteorological parameters of temperature, precipitation, wind speed, and the ENSO index in the statistical period of (1985-2014). They concluded that dust events had the highest correlation with temperature and the lowest correlation with precipitation. The relationship between dust events and ENSO also showed that El Niño was the dominant phenomenon in the first and second decades and La Niña in the last decade of the study period (Muslih et al. 2021). Huang et al. (2021) investigated the global impact of ENSO on dust activities from the Arabian Peninsula to Central Asia. Yang et al. (2022) investigated the impact of El Niño on dust in China during winter and spring and showed that there is dust augmentation in northern China during El Niño. Gao et al. (2022) investigated the relationship between the teleconnection pattern of the eastern Atlantic Ocean and the source of dust storms in North China from 1954 to 2021. Sun et al. (2022) investigated the effect of the Arctic Oscillation (AO) on dust frequency in the Eastern Middle East from 1974-2019. The results showed a negative correlation between the AO index and the frequency of dusty air in the north of the Arabian Peninsula and a positive correlation in the center and southwest of the Arabian Peninsula. Zhang et al. (2022) showed that the Pacific Decadal Oscillation (PDO) may play an important role in teleconnection with aeolian dust event occurrence in China.

Pourasghar et al. (2021) investigated the influence of the MJO on daily surface air temperature over Iran and found that

composites of daily surface air temperature anomalies are positive in MJO phases 1 and 8 and negative in MJO phases 3-4. Jamshidi Khezeli et al. (2022) investigated autumn and winter extreme precipitation events and their relationship with ENSO, NAO, and MJO Phases over the West of Iran and found that extreme precipitation occurred during moderate to strong El Niño. Almazroui. (2023) using the RMM index, investigated the effect of MJO on rainfall variability during November - April in Saudi Arabia and showed that 41% of rainfall during phases 3-6 have been occurred. Bao et al. (2022) tracked dust storms in China and Mongolia from March to June (2016-2020) using satellite imagery and the HYSPLIT model and found that dust storms originated in dry inland areas such as the Taklamakan and Gobi deserts were concentrated. Dargahian et al. (2023), using remote sensing techniques and the HYSPLIT model, identified the sources of dust in Khuzestan province (Iran) from 2003 to 2018 and showed that the lands of Iraq and Saudi Arabia have the most considerable role in the production of dust imported to the southwest of Iran.

Several studies have been conducted on the relationship between the MJO and climate elements such as monthly rainfall (Jani et al. 2022) and cyclonic storms (Paul et al. 2022), but little research has been conducted on the relationship between the MJO and dust storms. The researchers showed that the HYSPLIT model is suitable for tracking dust storms. Also, the results of researchers' studies showed that the MJO is effective in the frequency of dust storms. On the other hand, to monitor the MJO, a real-time multivariate MJO index (RMMI) is essential (Wheeler and Hendon 2004). Therefore, in the present study, the effect of the MJO on the frequency of dust storms at Sarpol-E-Zahab, Islamabad Gharb, Kermanshah, and Kangavar stations located in Kermanshah province

(as representative stations of the west of Iran) was investigated during a statistical period of 35 years 1987-2022. Since no study has been conducted on the effect of the MJO on dust occurrence in Iran, and most of the research has focused on the effect of other teleconnections, such as ENSO and NAO, it is necessary to investigate the effect of the MJO on the occurrence of dust storms.

2 Materials and methods

2.1 Study Area

Kermanshah province is located between latitude $33^{\circ} 40'$ to $35^{\circ} 18'$ north and longitude $45^{\circ} 24'$ to $48^{\circ} 07'$ east and has an average height of 1212 m above sea level. The geographical location of Iran and the stations of Kermanshah province are shown in Figure 1.

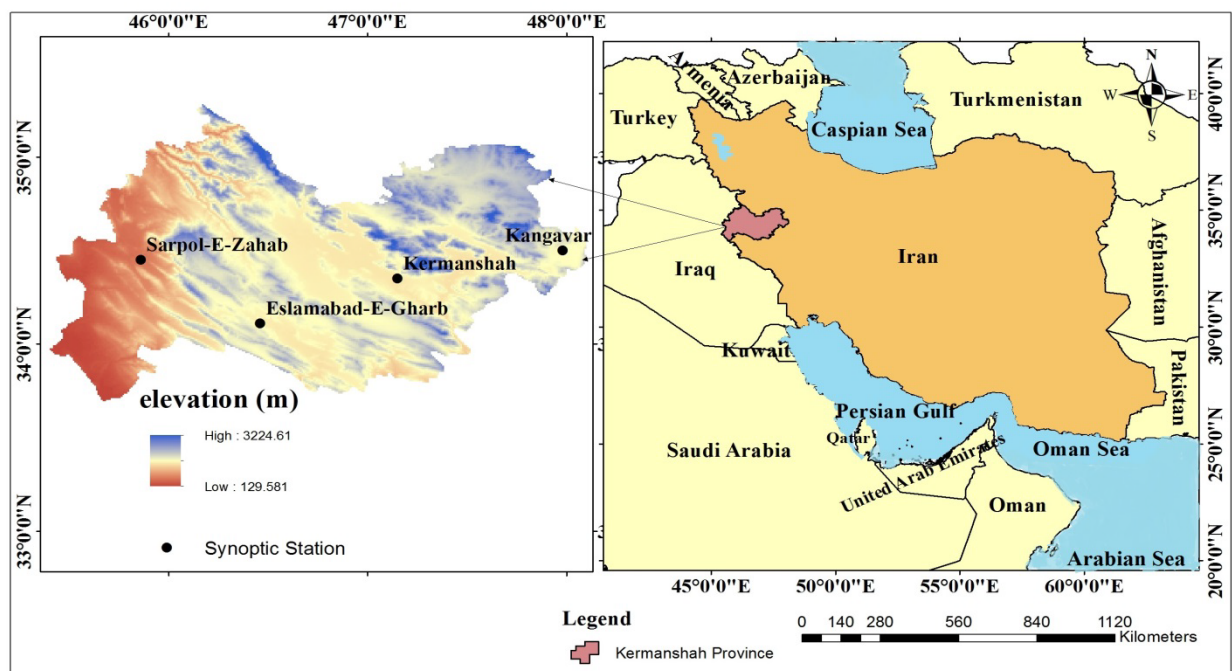


Figure 1. The geographical location of Kermanshah province and the studied synoptic stations.

Daily data related to horizontal visibility and present weather code for a statistical period of 35 years (1987-2022) were received from the Islamic Republic of Iran Meteorological Organization (IRIMO). Horizontal visibility data less than 1 km and dust phenomenon codes (6, 7, 8, 9, 30, 31, 32, 33, and 35) were filtered from codes 0 to 99 (Goudie and Middleton, 2006; Alizadeh-Choozari et al. 2016; Fattahi Masrouf and Rezazadeh, 2022; Liu et al. 2023). Then MJO data were obtained from the Australian Government Climate and Air Research Center (www.bom.gov.au/climate/mjo) and filtered for the statistical period of

February to July (1987-2022). The relationship between the RRM index and the frequency of dust storms in phases 7-2 (7, 8, 1, and 2), phases 3-6 (3, 4, 5, and 6), when its amplitude is ± 1 in four selected stations of Kermanshah province (Sarpol-E-Zahab, Islamabad Gharb, Kermanshah, and Kangavar) as representative stations of the west of Iran was investigated.

The RMM index was used to investigate the relationship between the MJO and the frequency of dust storms. Amplitude was used to evaluate the efficiency of MJO, which is defined by Equation 1 (Wheeler and Hendon 2004; Dee et al. 2011):

$$\text{Amplitude} = \sqrt{\text{RMM1}^2 + \text{RMM2}^2} \quad (1)$$

In this equation, these two-time series represent the first two components (PC1, PC2) of component analysis (PCs).

When the amplitude in each RMM phase is greater or equal to 1, the MJO phase is intense, and when this index is less than 1 the MJO phase is considered weak (Pai et al., 2011). The complete cycle of this phenomenon includes four positive phases (phases 3, 4, 5, and 6) and four negative phases (1, 2, 7, and 8). The RMM index uses Empirical Orthogonal Functions (EOF) analysis of Outgoing Longwave Radiation (OLR) difference, zonal wind at 850 hPa, and zonal wind at 200 hPa, which is averaged from 15°S to 15°N. The RMM index and other EOF based on techniques have several limitations, such as the need for long-term historical data (Straub, 2013).

To test the average dust storm difference (in terms of horizontal visibility) in phases 7-2 and phases 3-6 of the MJO of each station using the Mann-Whitney non-parametric test (Mann and Whitney 1947) in SPSS software, the significance of the difference in average dust storm data of each station compared to other stations was tested. This test shows in which stations there is a significant difference between the average dust storm in the es 7-2 and phases (3-6). To track the entry routes of dust storms that occurred in Kermanshah province, the days were selected when dust occurred in all study stations, and among these days, 4 representative days were selected in phases 7-2 and 3-6. Using the HYSPLIT model (backward model), dust storm particles were tracked at three levels of

200, 1000, and 1500 m from the ground in a time interval of 6 hours before the arrival of the dust storm. This model is a dual model for dust storm track calculations (Draxler et al. 2009). The calculation method of the model is a combination of Eulerian (total particle concentration for each grid is determined along the movement path) and Lagrangian (total particle concentration for each grid is determined using particle diffusion and transport movements) (Shan et al. 2009). The return paths show the Lagrangian path of the air parcel. Decreasing soil moisture causes the creation of dust centers, and its social and economic effects vary from small to large time and place (Wang, 2015). Therefore, in the continuation of this research, changes in soil moisture anomalies from zero to 10 cm above the soil along with wind vector anomalies at the level of 850 hPa (to investigate the direction of wind movement in active and weak states of phases 7-2 and 3-6) obtained from psl.noaa.gov/data/compositestest/printpage.pl website.

3 Results

3.1 Statistical results

Since the analyses showed that February to July comprised 45.79 to 81.39% of the annual dust occurrence (Table 1), therefore, the data were analyzed only for this statistical period (Nazemosadat et al. 2023). Table 1 shows the frequency and percentage of dust occurrence at selected stations of Kermanshah province for the statistical period under study.

Table 1 The frequency of dust storms in selected stations of Kermanshah province in the statistical period of 1987-2022

Stations	Dust frequency	The percentage of Feb to Jul dust storms
Eslamabad-E-Gharb	71	80.28
Sarpol-E-Zahab	264	80.30
Kermanshah	105	79.45
Kangavar	43	81.39

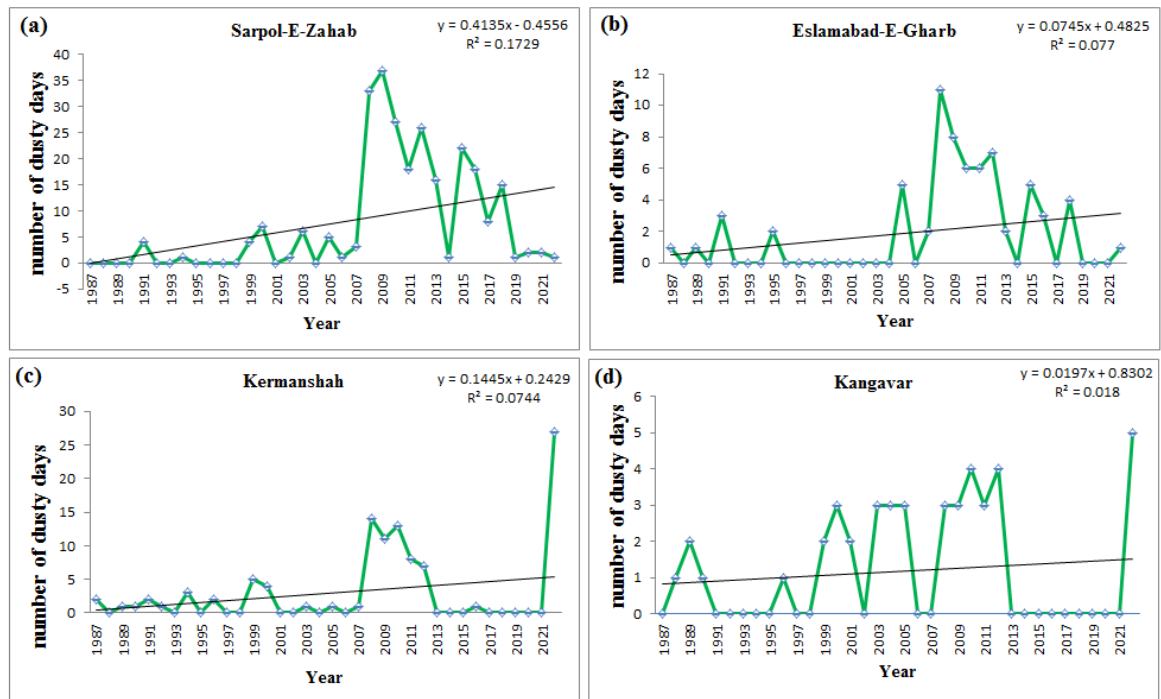


Figure 2. The annual frequency of dust storm days in selected stations of Kermanshah province in 1987-2022.

The frequency of dust storms in all stations shows significant annual changes (Figure 2a-d). From 1987 to 2005, the trend of increasing dust storms in Kermanshah province was not very noticeable, but from 2007 to 2013, it showed a significant increase. The highest frequency of dust storms related to Sarpol-E-Zahab and Islamabad Gharb stations were 40 and 12 storms recorded in 2008, respectively, the second amplification of the frequency of dust storms in 2021 was observed in Kermanshah and Kangavar so that in this year, the frequency of dust in Kermanshah station has reached 30 cases. Table (2) shows the results of the Mann-Whitney test to evaluate the significant difference in the average dust storms. The average dust storm based on the MJO shows a significant difference at the 95% confidence level in the Kangavar and Kermanshah stations, and no significant difference is observed the in Islamabad Gharb and Sarpol-E-Zahab stations. In fact, this test showed that if there is a difference between the averages, the

probability of a dust storm will be very high in the MJO.

Table 2. Comparison of dust storm averages with the MJO in the period 1985-2022.

Stations	Mann-Whitney test
Eslamabad-E-Gharb	0.789
Sarpol-E-Zahab	0.561
Kermanshah	0.059
Kangavar	0.035

The frequency of dust storms based on horizontal visibility of fewer than 1000 m and codes 6, 7, 8, 9, 30, 31, 32, 33, 34, and 35 in February, March, April, May, June, and July for (1987-2022) and for four selected stations of Kermanshah province is shown in Figure 3. Then, the ratio of the number of dust storm days to the total number of dusty days was calculated when the MJO was active and weak. Based on this, in phases 7-2 of the MJO, the highest probability of dust storms in Sarpol Zahab station was associated with 66% frequency and occurred when the MJO was in an active state and the range was

equal to or greater than one. Kermanshah, Kangavar, and, Islamabad-E-Gharb stations are in the following ranks of 56, 55, and 53%, respectively.

The lowest occurrence of dust storms was at the Sarpol-E-Zahab station with 34%; in this case, the MJO was in a weak and inactive state, and the amplitude was smaller than one (Figure 3-a). In the phases (3-6) of the MJO, the highest role of the index in the occurrence of dust related to Eslamabad-E-Gharb and Kangavar stations with 75 and 71%, respectively, belongs to the time when this index was in an active state. The decrement probability of dust occurrence at 52% is related to the Kermanshah station in the active state of this index and the Eslamabad-E-Gharb station with 25% in the weak state of this index (Figure 3-b).

When the MJO was in phases 7-2, 58 to 63% of the dust storms occurred in

Kermanshah province, and 37 to 42 % of the storms occurred in phases (3-6) of this index (Figure 3-c). In general, it can be said that the es 7-2 of the MJO account for a higher percentage of dust storms in Kermanshah than the es 7-2 of this index. The probability of dust storms in the active state of the MJO is higher than in its weak state, and its value fluctuates between 65% at Eslamabad-E-Gharb station and 52% at Kangavar station Figure (3-a-b). The percentage of occurrence of dust in the weak state of this index changes between 48% in Kangavar station and 34.6% in Eslamabad-E-Gharb station (Figure 3-d). By computing the function of phases 3-6 and phases 7-2 and amplitude amounts individually, it can be said that phases 7-2 and amplitude greater than or equal to 1 are more necessary and effective in the incidence of dust storms in the stations of Kermanshah province.

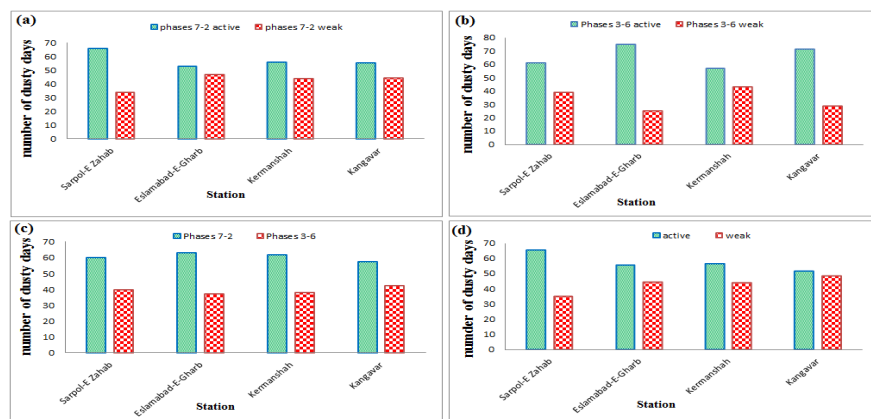


Figure 3. The percentage of occurrence of dust storms in Kermanshah province in the active and weak states of phases 7-2 and 3-6 of the MJO.

3.2. Tracking the path of the dust storm

Tracking the path of the dust storm with the backward method at different levels showed that during the prevailing phases 7-2 of the MJO, which includes 30 days of the total number of dust events (18 active days and 12 weak days), the path of dust entering Kermanshah province was from Iraq and eastern Syria. To track the path of dust storms in active and weak phases, 4 days of MJO were selected as the

representative for of Kermanshah, Islamabad Gharb, and Sarpol-E-Zahab (Table 3). Considering the output of the HYSPLIT model, the primary source of dust particle transmission to Kermanshah province in phases 7-2 of the MJO was an area between Iraq and the eastern parts of Syria. The paths of particles transfer at three levels of 200, 1000, and 1500 m area function of the direction of the west winds, and the smoother the ground, the waste the

soil moisture, and the drier the air, the more likely dust storms will occur. The tracking of dust particles entering Kermanshah province in phases 3-6 of the MJO indicates the movement of these particles from the eastern part of Iraq toward Khuzestan province and the movement of these particles from Khuzestan province toward Kermanshah province (Figure 4a-d).

When phases 3-6 of the MJO prevailed, the frequency of dust storms significantly decreased compared with phases 7-2 in Kermanshah province, and its number reached 17 (11 active days and 6 weak days). Tracking the path of dust particles

entering Kermanshah province in these 17 days indicates the movement of these particles from the eastern part of Iraq to Khuzestan province in Iran and the movement of these particles from Khuzestan province to Kermanshah province, which confirms the direction of movement of this path in the selected days of phases 3-6 in the active and inactive states of the index in table (3). It can be said that in phases 3-6, in addition to external sources, domestic sources have been effective in the occurrence of dust storms in Kermanshah province (Figure 5a-d).

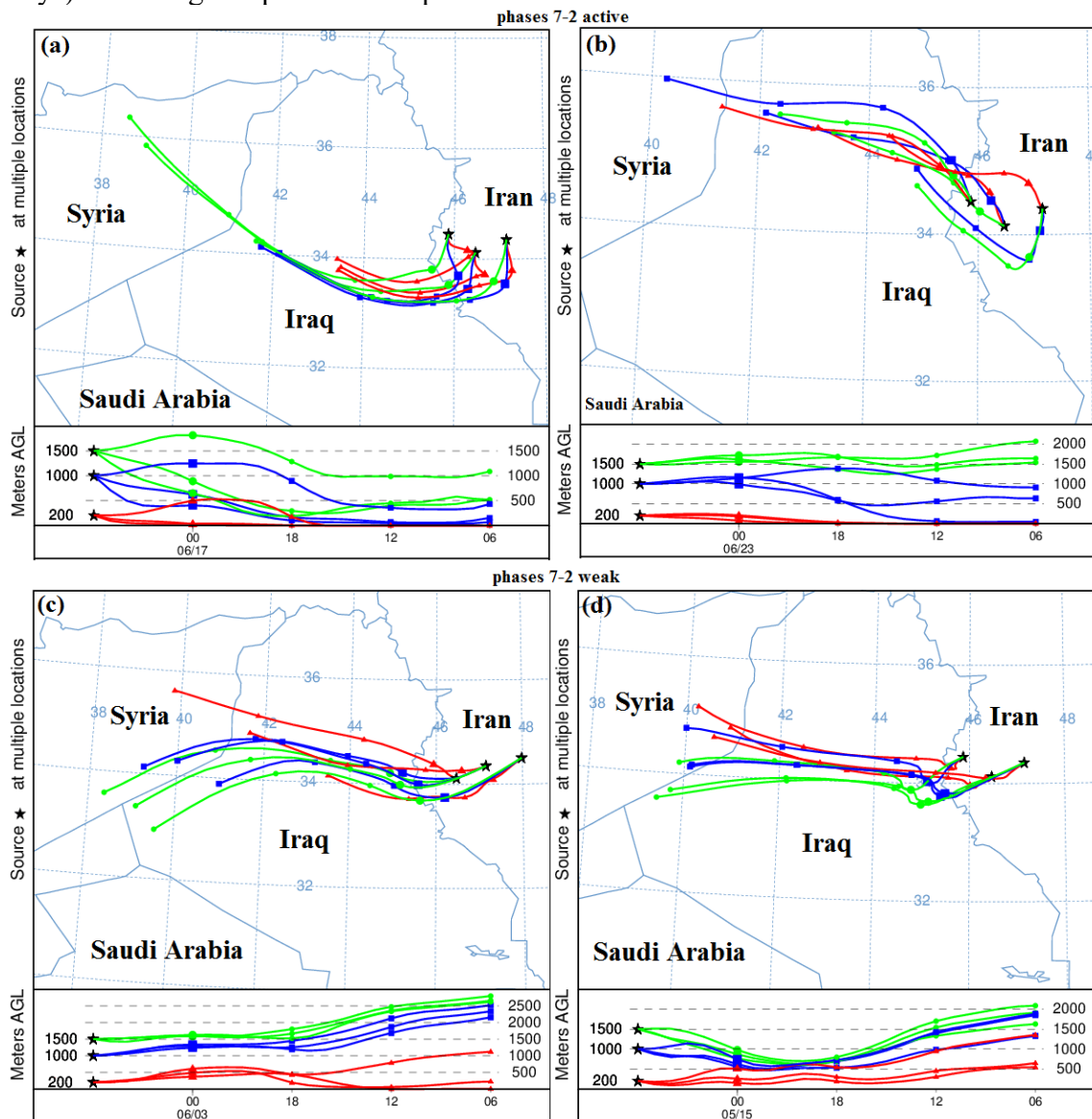


Figure 4. Dust particle tracking with the HYSPLIT model
 a) 06.17.2016 b) 06.23.2018 c) 06.03.2011 d) 05.15.2012

Table 3. Selected days to track the entry path of dust storms to Kermanshah Province with the HYSPLIT model

Figure	Date	Phase
5-a	06.17.2016	Phases 7-2 Active
5-b	06.23.2018	
5-c	06.03.2011	
5-d	05.15.2012	
6-a	04.05.2011	Phases 3-6 Active
6-b	02.19.2022	
6-c	04.17.2008	Phases 3-6 Weak
6-d	02.01.2022	

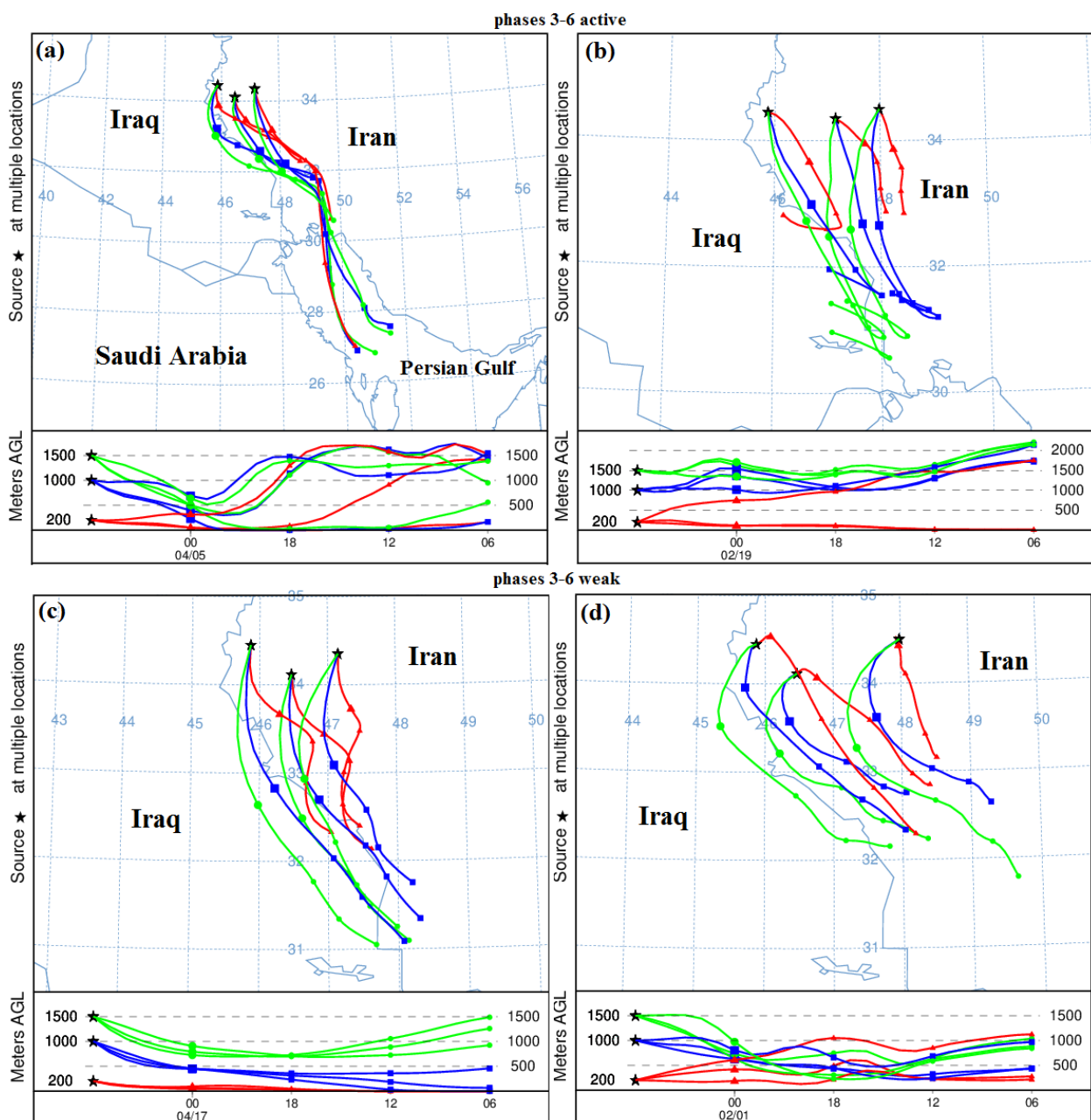


Figure 5. Dust particle tracking with the HYSPLIT model
 a) 04.05.2011 b) 02.19.2022 c) 04.17.2008 d) 02.01.2022

3.3 Analysis of 850 hPa level wind maps

The difference of the vector wind at the 850 hPa level compared to the long-term average of phases 7-2 and phases 3-6 of the MJO is shown in Figure (6a-d). It was founded simultaneously with the dominance of phases 7-2 and phases 3-6 in two active and weak states of these phases, the wind direction is circular and from the west (Zonal Wind), which is associated with an increase in the speed of the

westerly winds over Iraq, Syria, and Turkey. In areas such as Iraq, Syria, and Saudi Arabia, the severe decrease in soil moisture has caused the movement of dry air masses along with dust storms to the western regions of Iran, and tracking the path of dust entering Kermanshah province with the HYSPLIT model also confirmed the entry of dust from these areas into Kermanshah province.

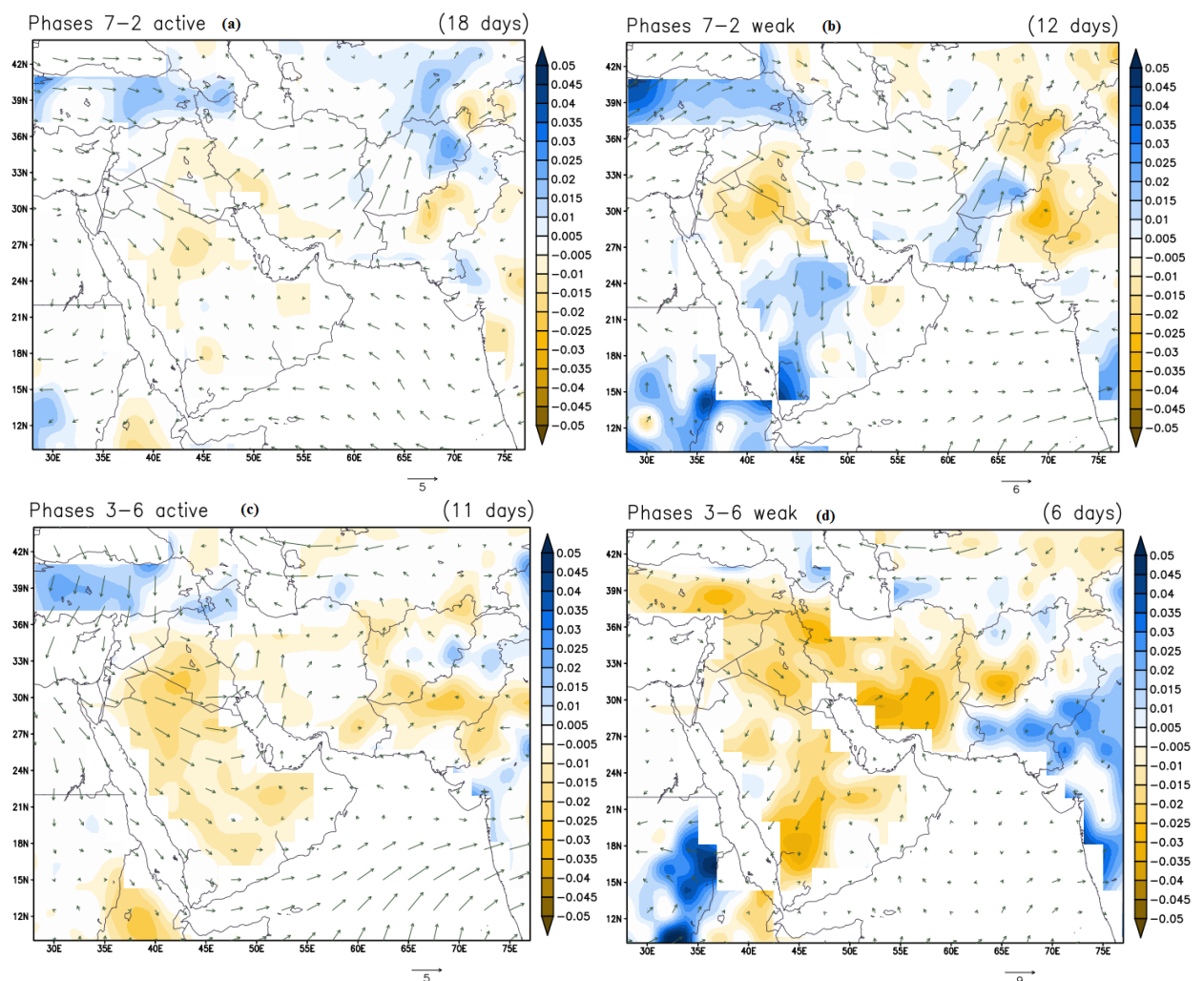


Figure 6. Composite Anomaly of soil moisture and 850 hPa level vector wind in active and weak states of phases 7-2 and phases 3-6 of the MJO. The areas in blue (brown) color shades show the increase (decrease) in soil moisture compared to the long-term average (1991-2020) at the level of 0-10 cm, and the vectors show the direction and wind speed of the 850 hPa level compared to the long-term average in based on (m/s).

4. Conclusion

To investigate the effect of the MJO on the frequency of dust storms in 4 selected stations of Kermanshah province (as representative stations of the west of Iran),

the days with dust storms were determined according to the horizontal visibility below 1000 m, and the codes related to dust storms during a statistical period of 35 years. The results of the Mann-Whitney

test showed that in terms of the average occurrence of dust storms, Sarpol-E-Zahab and Islamabad Gharb stations are not statistically significantly different, but Kangavar and Kermanshah stations have statistically significant differences from each other in terms of the average occurrence of dust storms in 6 months of the year (February - July). The results obtained from examining the frequency of dust occurrence in phases 7-2 and phases 3-6 of the MJO showed that when the rate of the MJO is greater or equal to 1, and the index is in the active state, the amount of dust occurrence in the province Kermanshah is more than when the intensity of the MJO is low, weak, and inactive. Generally, the MJO in its phases 7-2 justifies a higher percentage of dust occurrences in Kermanshah than in phases 3-6. The highest percentage of dust occurrence is in Islamabad Gharb station with about 62% in the es 7-2, and the lowest is in Kermanshah station, with 38% in the phases 3-6 of the MJO. The research of Yu and Ginoux (2021) showed that in Australia, the peak of dust activity during phases 1- 6 of the MJO oscillation is associated with El Niño activity. This result is consistent with the findings of this research. Tracking the paths of dust entering Kermanshah province with the HYSPLIT model at three levels of 200, 1000, and 1500 m showed that the primary source of dust particles entering Kermanshah province is from eastern Syria and Iraq.

5 References

- Ahmadi Doabi, S., Afyuni, M., and Karami, M., 2017, Multivariate statistical analysis of heavy metals contamination in atmospheric dust of Kermanshah province, western Iran, during the spring and summer 2013: *Journal of Geochemical Exploration*, 3-28. <https://doi.org/10.1016/j.gexplo.2017.06.007>.
- Ahn, M.S., Kim, D., Kang, D., Lee, J., Sperber, K.R., Gleckler, P.J., Xianan, J., Yoo-Geun, H., and Hyemi, H., 2020, MJO propagation across the Maritime continent: Are CMIP6 models better than CMIP5 models?: *Geophysical Research Letters*, 47. <https://doi.org/10.1029/2020gl087250>.
- Alizadeh-Choobari, O., Ghafarian, p and Owlad, E., 2016, Temporal variations in the frequency and concentration of dust events over Iran based on surface observations: *International Journal of Climatology*, 36, 2050–2062. DOI: 10.1002/joc.4479.
- Almazroui, M., 2023, The Influence of the Madden–Julian Oscillation on the Wet Season Rainfall over Saudi Arabia: *Earth Systems and Environment*, 7, 1–14.
- Azizi, G., Shamsipour, A.A., Miri, M., and Safarrad, T., 2012, Statistic and synoptic analysis of dust phenomena in west of Iran: *Journal of Environmental Studies*, 38(63), 31-33. DOI:10.22059/JES.2012.29154.
- Banerjee, P., Kumar, S.P., 2016, ENSO Modulation of Interannual Variability of Dust Aerosols over the Northwest Indian Ocean: *Journal of Climate*, 29(4), 1287-1303. DOI:10.1175/JCLI-D-15-0039.1.
- Bao, C., Yong, M., Bueh, C., Bao, Y., Jin, E., Bao, Y., and Purevjav, G., 2022, Analyses of the Dust Storm Sources, Affected Areas, and Moving Paths in Mongolia and China in Early Spring: *Natural Disaster Risk Assessment and Management Using Remote Sensing Techniques*, 14(15), 3661. <https://doi.org/10.3390/rs14153661>.
- Chauhan, A., Samara, C., and Sing, R.P., 2018, Pronounced changes in air quality, atmospheric and meteorological parameters, and strong mixing of smoke associated with a dust event over Bakersfield, California: *Environmental Earth Sciences*, 77(4), 115. <http://dx.doi.org/10.1007/s12665-018-7311-z>.

- Dargahian, F., Mousivand, Y., Razavizadeh, S., and Lotfinasabasl, S., 2023, Identifying Dust Sources Affecting Southwestern Iran (Khuzestan Province) Using Remote Sensing Techniques and HYSPLIT Model: *Journal of the Indian Society of Remote Sensing*, **51**, 565-583. <https://doi.org/10.1007/s12524-022-01648-y>.
- Dee, D.P., Uppala, S.M., Simmons, A.J., Berrisford, P., Poli, P., Kobayashi, S., Andrae, U., Balmaseda, M.A., Balsamo, G., Bauer, P., Bechtold, P., Beljaars, A.C.M., van de Berg, L., Bidlot, J., Bormann, N., Delsol, C., Dragani, R., Fuentes, M., Geer, A.J., Haimberger, L., Healy, H., Hersbach, S.B., Hólm, E.V., Isaksen, L., Kállberg, P., Köhler, M., Matricardi, M., McNally, A.P., Monge-Sanz, B.M., Morcrette, J.J., Park, B.K., Peubey, C.P., Rosnay, D., Tavolato, C., Thépaut, J.N., and Vitart, F., 2011, The ERA-Interim reanalysis: Configuration and performance of the data assimilation system. *Quart: Journal Of the Royal Meteorological Society*, **137**, 553–597. <https://doi.org/10.1002/qj.828>.
- Draxler, R., Stunder, B., Rolph, G., Stein, A., and Taylor, A., 2009, HYSPLIT4 user's guide, Version 4.9:1-231.
- Farhadipour, S., Azadi, M., Bidokhti, A.A., Sayyari, H., and Alizadeh Choobari, O., 2018, Study and Simulation of Severe Dust Storms in the West and Southwest of Iran: *Russian Meteorology and Hydrology*, **43**, 613–624. <https://doi.org/10.3103/S106837391809008X>.
- Fattahi Masrou, P., and Rezazadeh, M., 2022, Spatio-Temporal Distribution of Various Types of Dust Events in the Middle East during the Period 1996-2015: *Journal of the Earth and Space Physics*, **47(4)**, 231-248. DOI: 10.22059/JESPHYS.2021.321010.1007306/.
- Gao, T., Han, J., Wang, Y., Pei, H., and Lu, S., 2012, Impacts of climate abnormality on remarkable dust storm increase of the Hunshdak Sandy Lands in northern China during 2001–2008: *Meteorological Applications*, **19(3)**, 265–278. <https://doi.org/10.1002/met.251>.
- Gao, T., Chang, A., Jing, Ma, M.Y., Yang, Z., and Yu, X., 2022, Relationship between the East Atlantic teleconnection pattern and the spring dust storm in northern China: *Meteorological Applications*, **29**, 1-21. <https://doi.org/10.1002/met.2085>.
- Gong, D.Y., Mao, R., and Fan, Y.D., 2006, East Asian dust storm and weather disturbance: possible links to the Arctic Oscillation: *International Journal of Climatology*, **26(10)**, 1379-1396. <https://doi.org/10.1002/joc.1324>.
- Gong, D.Y., Mao, R., Shi, P.J., and Fan, Y.D., 2007, Correlation between east Asian dust storm frequency and PNA: *Journal of Geophysical Research Letters*, **34(14)**. DOI:10.1029/2007GL029944.
- Goudie, A., Middleton, N., 2006, *Desert dust in the global system*. New York: Springer Berlin Heidelberg
- Gui, K., Yao, W., Che, H., An, L., Zheng, Y., Li, L., Zhao, H., Zhang, L., Zhong, J., Wang, Y., and Zhang, X., 2022, Record-breaking dust loading during two mega dust storm events over northern China in March 2021 aerosol optical and radiative properties and meteorological drivers: *Atmospheric Chemistry and Physics*, **22(12)**, 7905-7932. <https://doi.org/10.5194/acp-22-7905-2022>.
- Guo, Y., Tian, B., Kahn, R.A., Kalashnikova, O., Wong, S., and Waliser, D.E., 2013, Tropical Atlantic dust and smoke aerosol variations related to the Madden-Julian Oscillation in MODIS and MISR observations: *Journal of Geophysical*

- Research Letters: Atmospheres, **118(10)**, 4947–4963. <https://doi.org/10.1002/jgrd.50409>.
- Hung, M.P., Lin, J.L., Wang, W., Kim, D., Shinoda, T., and Weaver, S.J., 2013, MJO and convectively coupled equatorial waves simulated by CMIP5 climate models: *Journal of Climate*, **26(17)**, 6185–6214. <https://doi.org/10.1175/JCLI-D-12-00541.1>.
- Huang, Y., Liu, X., Yin, Z. Y., and An, Z., 2021, Global impact of ENSO on dust activities with emphasis on the key region from the Arabian Peninsula to Central Asia: *Journal of Geophysical Research: Atmospheres*, **126**, e2020JD034068. <https://doi.org/10.1029/2020JD034068>.
- Jamshidi Khezeli, T., Ranjbar Saadat Abadi, A., Nasr-Esfahany, M. A., Tajbakhsh Mosalman, S., and Mohebalhojeh, A.R., 2022, Autumn and Winter Extreme Precipitation Events and their Relationship with ENSO, NAO and MJO Phases over the West of Iran: *Journal of the Earth and Space Physics*, **47(4)**, 201-218. DOI: 10.22059/JESPHYS.2021.316961.1007280.
- Johny, K., Pai, M.L., and Adarsh, S., 2022, Investigating the multiscale teleconnections of Madden-Julian oscillation and monthly rainfall using time-dependent intrinsic cross-correlation: *Natural Hazards*, **112(2)**, 1795–1822. DOI: 10.1007/s11069-022-05249-3.
- Pourasghar, F., Oliver, E. C. J., and Holbrook, N. J. 2021, Influence of the MJO on daily surface air temperature over Iran: *Journal of Climatology*, 1-12. DOI: 10.1002/joc.7086.
- Karimi, M., Oladi Ghadikolaei, J., and Mohammadi, J., 2018, Identification of dust storm sources area using Ackerman index in Kermanshah province, Iran: *Journal of Research in Biology*, **8(6)**, 2534-2543.
- Labban, A., Butt, M.J., 2021, Analysis of sand and dust storm events over Saudi Arabia in relation with meteorological parameters and ENSO: *Arabian Journal of Geosciences*, **14(22)**. <https://doi.org/10.1007/s12517-020-06291-w>.
- Lee, Y.G., Kim, J., Ho, C.H., An, S.I., Mao, R., Tian, B., Wu, D., Lee, J.N., Kalashnikova, O., Choi, Y., and Yeh, S.W., 2014, The effects of ENSO under negative AO phase on spring dust activity over northern China: An observation investigation: *International Journal of Climatology*, **35(6)**, 935-947. DOI:10.1002/joc.4028.
- Li, J., Garshick, E., Huang, S., and Koutrakis, P., 2021, Impacts of El Niño-Southern Oscillation on surface dust levels across the world during 1982–2019: *Science of The Total Environment*, 769. DOI: 10.1016/j.scitotenv.2020.144566.
- Ling, J., Zhang, C., Wang, S., and Li, C., 2017, A new interpretation of the ability of global models to simulate the MJO: *Geophysical Research Letters*, **44(11)**, 5798–5806. DOI: 10.1002/2017GL073891.
- Ling, J., Zhao, Y., and Chen, G., 2019, Barrier effect on MJO propagation by the Maritime continent in the MJOTF/GASS models: *Journal of Climate*, **32(17)**, 5529–5547. <https://doi.org/10.1175/JCLI-D-18-0870.1>.
- Liu, X., Zhang, Y., Yao, H., Lian, Q., and Xu, J., 2023, Analysis of the Severe Dust Process and Its Impact on Air Quality in Northern China: *Atmosphere*, **14(7)**, 1071; <https://doi.org/10.3390/atmos14071071>.
- Mann, H.B., Whitney, D.R., 1947, On a test of whether one of 2 random variables is stochastically larger than the other. *Ann Math Stat*, 18, 50- 60.

- Mei, D., Xiushan, L., Sun, L., and Ping, W., 2008, A dust-storm process dynamic monitoring with multi-temporal MODIS data: *Int Arch Photogram Remote Sens Spat Inf Sci*, **6**, 965–970.
- Mesbahzadeh, T., Salajeghe, A., and Sardoo, F.S., 2020, Climatology of dust days in the Central Plateau of Iran: *Natural Hazards*, **104**, 1801–1817. <https://doi.org/10.1007/s11069-020-04248-6>
- Muslih, K.D., Umran, T.A., and Shiltagh, A.G., 2021, Analysis of Correlation and Coupling between El Niño-Southern Oscillation and Dust Storms in Iraq from 1971 to 2016: *Iraqi Geological Journal*, **54**, 103-113. DOI: 10.46717/igj.54.1E.9Ms-2021-05-30.
- Nazemosadat, M.J., Shahgholian, K., and Ghaedamini, H., 2023, The wet and dry spells within the MJO-phase 8 and the role of ENSO and IOD on the characteristics of these spells: A regional to continental-scales analysis: *Atmospheric Research*. <http://dx.doi.org/10.2139/ssrn.4188407>.
- Pai, D.S., Bhate, J., Sreejith, O.P., and Hatwar, H.R., 2011, Impact of MJO on the intraseasonal variation of summer monsoon rainfall over India: *Climate Dynamics*, **36(1)**, 41–55. DOI: 10.1007/s00382-009-0634-4.
- Paul, D., Panda, J., and Routray, A., 2022, Ocean and atmospheric characteristics associated with the cyclogenesis and rapid intensification of NIO super cyclonic storms during 1981–2020: *Natural Hazards*, **114(1)**, 261–289. <https://doi.org/10.1007/s11069-022-05389-6>
- Ragsdale, K.M., Bradford Barrett, S., and Testino, A.P., 2013, Variability of particulate matter (PM 10) in Santiago, Chile by phase of the Madden-Julian Oscillation (MJO): *Atmospheric Environment*, **81**, 304–310. DOI:10.1016/j.atmosenv.2013.09.011.
- Saeed, T.M., Al-Dashti, H., and Spyrou, C., 2014, Aerosol's optical and physical characteristics and direct radiative forcing during a shamal dust storm, a case study: *Atmospheric Chemistry and Physics*, **14(7)**, 3751–3769. <https://doi.org/10.5194/acp-14-3751-2014>.
- Salahi, B., Vatanparast Ghaleh Juq, F., and Nazari Radsani, M., 2024. Evaluating the Effects of Climate Change on MJO-Related Precipitation in the Southern Coast of Iran. *Amphibious Science and Technology*, DOI:10.22034/jamst.2024.544421.1154
- Shan, W., Yin, Y., Lu, H., and Liang, S., 2009, A meteorological analysis of ozone episodes using HYSPLIT model and surface data: *Atmospheric Research*, **93(4)**, 767–776. DOI: 10.1016/j.atmosres.2009.03.007.
- Shao, Y., Wyrwoll, K.H., Chappell, A., Huang, J., Lin, Z., McTainsh, G.H., Mikami, M., Tanaka, T.Y., Wang, X., and Yoon, S., 2011, Dust cycle: an emerging core theme in earth system science: *Aeolian Research*, **2**, 181–204. DOI:10.1016/j.aeolia.2011.02.001.
- Straub, K.H., 2013, MJO initiation in the Real-time Multivariate MJO index: *Journal of Climate*, **26(4)**, 1130–1151. <https://doi.org/10.1175/JCLI-D-12-00074.1>.
- Sun, Y., Mao, R., Gong, D.Y., Li, Y., Kim, S.J., Zhang, X.X., Zhang, X., and Hamidi, M., 2022, Decadal shift of the influence of Arctic Oscillation on dust weather frequency in spring over the Middle East during 1974–2019: *International Journal of Climatology*, **42(4)**, 2440-2454. <https://repository.kopri.re.kr/handle/201206/13321>.
- Wang, J. X., 2015, Mapping the global dust storm records: Review of dust data sources in supporting modeling/climate study: *Current Pollution Reports*, **1(2)**,

- 82-94. DOI: 10.1007/s40726-015-0008-y.
- Wheeler, M., Hendon, H., 2004, An all-season real-time multivariate MJO index, Development of an index for monitoring and prediction: *Monthly Weather Review*, **132(8)**, 1917-1932. [https://doi.org/10.1175/1520-0493\(2004\)132<1917:AARMMI>2.0.CO;2](https://doi.org/10.1175/1520-0493(2004)132<1917:AARMMI>2.0.CO;2).
- Xu, J., Hou, S., Qin, D., Kang, S., Ren, J., and Ming, J., 2007, Dust storm activity over the Tibetan Plateau recorded by a shallow ice core from the north slope of Mt. Qomolangma (Everest), Tibet-Himal region: *Journal of Geophysical Research Letters*, **34(17)**. DOI: 10.1029/2007GL030853.
- Yang, Y., Zeng, L., Wang, H., Wang, P., and Liao, H., 2022, Dust pollution in China affected by different spatial and temporal types of El Niño: *Atmospheric Chemistry and Physics*, **22**, 14489–14502. <https://doi.org/10.5194/acp-22-14489-2022>.
- Yong, L., Guangpeng, W., Ziyang, H., Peijun, S., Yanli, L., Guoming, Z., Yu, G., Yun, L., Chang, H., Lanlan, G., Xia, H., Yanyan, Y., Xiaoxiao, Z., Hao, Z., and Lianyou, L., 2020, Dust storm susceptibility on different land surface types in arid and semi-arid regions of northern China: *Atmospheric Research*, **243**. <https://doi.org/10.1016/j.atmosres.2020.105031>.
- Yu, Y., Ginoux, P., 2021, Assessing the contribution of the ENSO and MJO to Australian dust activity based on satellite- and ground-based observations: *Atmospheric Chemistry and Physics*, **21(11)**, 8511–8530. <https://doi.org/10.5194/acp-21-8511-2021>.
- Zhang, C., 2005, Madden-Julian Oscillation: *Reviews of Geophysics*, **43(2)**. <https://doi.org/10.1029/2004RG000158>.
- Zhang, C., 2013, Madden–Julian oscillation: Bridging weather and climate: *Bulletin of the American Meteorological Society*, 94(12),1849–1870. <https://doi.org/10.1175/bams-d-12-00026.1>.
- Zhang, X., Lei, J. Q., Wu, S. X., Li, S. Y., Liu, L. Y., Wang, Z. F., Huang, Sh. Y., Guo, Y. H., Wang, Y. D., Tang, X., and Zhou, j., 2022, Research Article, Spatiotemporal evolution of aeolian dust in China: An insight into the synoptic records of 1984–2020 and nationwide practices to combat desertification, 2005- 2023. DOI: 10.1002/ldr.4585.